Basrah Journal for Engineering Sciences, Vol. 22, No. 1, (2022), 78-85

Original Article

Journal homepage: www.bjes.edu.iq
ISSN (Online): 23118385, ISSN (Print): 18146120

OPEN ACCESS

Compact Low-Cost Reconfigurable Microwave Bandpass Filter Using Stub-Loaded Multiple Mode Resonator for WiMAX, 5G and WLAN Applications

Yousif Mohsin Hasan [1,*], Abdulkareem Swadi Abdullah [2], Falih Mahdi Alnahwi [3]

[1] *Department of Electronic and Communication, College of Engineering, University of Al-Qadisiyah, Al-Qadisiyah, Iraq*
[2,3] *Department of Electrical Engineering, College of Engineering, University of Basrah, Basrah, Iraq*
E-mail addresses: yousif.hasan@qu.edu.iq , abdulkareem.abdullah@uobasrah.edu.iq , falih.mousa@uobasrah.edu.iq
Received: 2 September 2021; Accepted: 10 November 2021; Published: 24 April 2022

Abstract

This paper presents a compact, low-cost reconfigurable bandpass filter (BPF) for WiMax, 5G, and WLAN applications. The BPF consists of a half-wavelength resonator folded as C-shaped by a pair of symmetrical PIN diodes and a central quarter-wavelength resonator to form an E-shaped stub-loaded multiple-mode resonator (SL-MMR). The feed line is made of two subsections separated by a gap which acts as a fixed capacitance and allows the filter to have bandpass behavior. The proposed filter is modeled using the even and odd mode analysis to predict the locations of the resonant frequencies. The simulation results show that the filter covers the frequency range (3.38-3.95) GHz with a center frequency of 3.52 GHz at the ON state of a pair of PIN diodes. On the other hand, the BPF covers the frequency range (4.7-5.93) GHz with a center frequency of 5.2 GHz, at the OFF state of the diodes. The results also show a small insertion loss at the filter passband with two sharp transmission zeros at the stopband.

Keywords: E-shaped filter, Reconfigurable BPF, SL-MMR filter, WiMAX, 5G, WLAN.

http://dx.doi.org/10.33971/bjes.22.1.9

1. Introduction

Electronically controlled reconfigurable bandpass filters are in great demand for wireless communication and cognitive radio systems due to their ability to achieve frequency tunable, compact filter-size, and simple construction. In addition, bandpass filters should have a multi-frequency response to satisfy the increasing demands of modern multifunctional communication systems. Reconfigurable bandpass filters (BPF) can adjust the spectrum of proposed wireless communication bands and provide support for cognitive radio systems [1], [2]. Several planar filters with varying performance levels have been investigated and applied in order to get different characteristics, such as the ultra-wide band (UWB) filter with stopband using parallel-coupled microstrip lines [3], the lowpass filter (LPF) [4], the tunable high pass filter (HPF) [5], and the bandpass filter (BPF) loaded with stepped impedance stubs [6].

Reconfigurable bandpass filters may be created and divided into two main kinds, namely discrete-switching or tuned filters and continuously-switching filters. PIN diodes, micro-electromechanical systems (MEMS) switches, or optical switches are commonly used in filter topologies with discrete switching. Filter designs based on varactor diodes, ferroelectric/magnetic materials, or MEMS capacitors are often used to enable continuous tuning [7]. Several design approaches for reconfigurable continuously tuning filter responses have been developed, such as [8] using two varactor diodes incorporated within a bandpass filter to get a frequency tuning range from 2.5 GHz to 3.8 GHz, and [9] also using varactor diodes integrated with T-shaped and H-shaped filters to achieve a 32.9 % frequency tuning range from 4.26 GHz to 5.94 GHz and with 36.7 % frequency TR from 3.85 GHz to 5.58 GHz, respectively. In [5], the implemented filter is found to have a continuous tuning range of 1030 MHz to 2150 MHz by using varactor diodes. Reference [10] achieves a high-selectivity tunable balanced BPF with a tuning range of 1.6 GHz to 2.27 GHz and a fractional bandwidth (FBW) of 34.6%. On the other hand, different methods for designing configurable discrete states for filter response have been developed, such as [11], the filter can change its bandpass behavior due to the change in the electrical length of the T-shaped slot using four PIN diodes. A reconfigurable SBF with a series of spiral resonators based on the PIN diodes is used in [12], and a switchable dual-band BPF is used in [13]. A ring resonator BPF with reconfigurable bandwidth based on a parallel-coupled line structure and a cross-shaped resonator with open stubs is presented in [14], and a wideband BPF with reconfigurable bandwidth (BW) is presented in [15]. A dual-mode microstrip square-loop resonator is used to design a reconfigurable BPF with switchable BW for wireless applications is proposed in [16]. In [17], a novel reconfigurable BPF for WiMAX and WLAN applications is proposed. Reconfigurable discrete-switching tuning using PIN diode technology has achieved particular interest over the reconfigurable continuously tuning filter using a varactor

diode due to its low RF loss and signal distortion, especially in the case of wide bandwidth where extensive tuning is required.

In addition, the PIN diode offers high power handling, fast switching speed at low cost, easier packing, and lower bias voltage [7]. Many studies have proposed the design of compact microwave bandpass filters through the use of the Multiple Mode Resonator (MMR) [12-15]. Stub loaded-MMR was used to design a microwave filter with improved passband and stopband characteristics for 5G applications [18]. The MMR was also used to generate a multi-band passband filter response [19], and the slot line version of the MMR was used to design a differential wideband BPF [20]. A quarter-wavelength resonator was attached to the MMR to generate electric and magnetic coupling in order to obtain multiple passbands [21]. Varactor diodes have been used to reconfigurable and tune the filter's pass band with MMR [22].

This paper presents a compact low-cost reconfigurable BPF for WiMAX, 5G and WLAN applications. A pair of PIN diodes is used with the aid of SL-MMR BPF to switch the filter frequency response discretely. At the ON state of the PIN diodes, the filter frequency coverage extends along the range of 3.38-3.95 GHz, centered at 3.52 GHz with a reflection coefficient less than -43 dB. On the other hand, the BPF covers the frequency range from 4.423 GHz to 6 GHz with a center frequency of 5.2 GHz and a reflection coefficient of less than -28 dB at the OFF state of the pair of the PIN diodes. For cost reduction objectives, the FR4 dielectric material is chosen as the dielectric substrate material of the proposed filter.

2. Reconfigurable E-shaped band-pass filter

The proposed E-shaped filter consists of a half-wavelength microstrip resonator and a central quarter-wavelength short-circuit stub as an SL-MMR that provides a nearly flat pass band and a pair of transmission zeros for improved stopband suppression. The low-cost FR4 substrate with a dielectric constant of 4.3, a loss tangent of 0.025, and a thickness of 16 mm is used as the substrate of the band pass filter structure. The top layer of the band pass filter has a feeding strip-line with a length of L_f = 17 mm and a width of W_f = 3 mm, providing a characteristic impedance of 50 Ω. The feed line consists of two subsections separated by a distance of W_{cut} = 0.2 mm gap. This gap operates as a fixed capacitance, allowing the filter to operate in band pass behavior [11]. The two strip-lines are coupled with an E-shaped, which is made up of a folded half-wavelength microstrip resonator and a short-circuit stub in the middle [23], [24]. The length of the microstrip resonator is L_1 = 14.3 mm, and the width is W_1 = 0.36 mm. The half-wavelength resonator is folded at both ends to reduce the size of the BPF. For reconfigurable BPF, a pair of PIN diodes for discrete switching is inserted into the folded region of the half-wavelength resonator. The central short circuit sub has a length of L_2 = 0.8 mm and a width of W_2 = 1 mm with a via hole of 0.5 mm diameter as shown in Fig. 1. The filter has total dimensions of length L_f and width W_g of (17 × 17) mm^2, which is 0.36 λ_g × 0.36 λ_g = 0.1297 λ_g^2 at a center frequency of 3.52 GHz. The bandpass filter can change its operating frequency by changing the length of the E-shaped microstrip resonator. The physical structure of the BPF with a metallic ground plane is shown in Fig. 1. All the dimensions of the proposed design are listed (in mm) in Table 1.

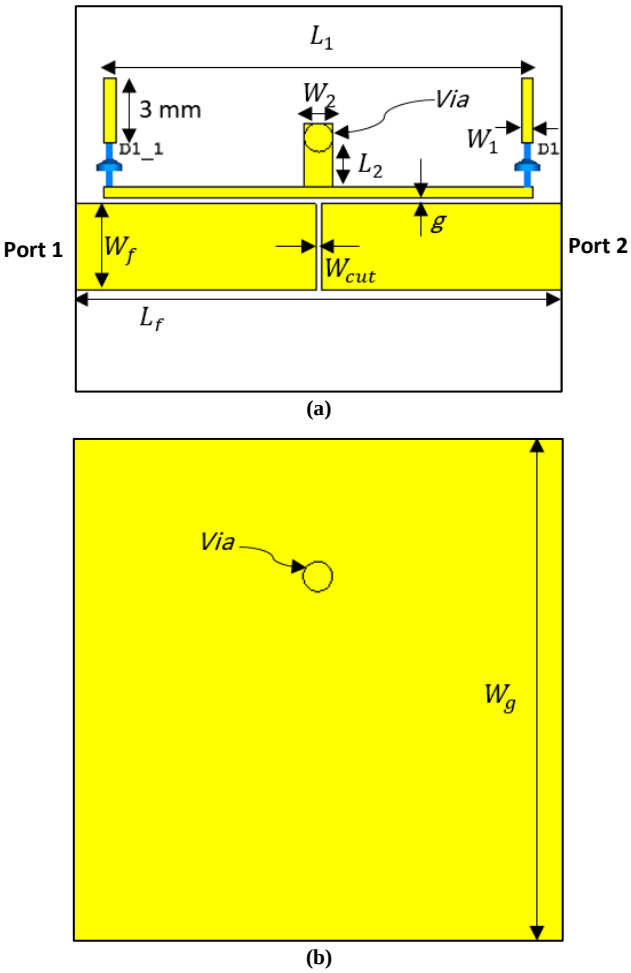

Fig. 1 Structure of proposed SL-MMR filter **(a)** Top view and **(b)** ground plane.

Table 1. Parameters value of the proposed BPF filter (in mm).

Width	Length	Gap and Via hole
W_f = 3	L_1 = 14.3	g = 0.2
W_1 = 0.36	L_2 = 0.8	W_{cut} = 0.2
W_1 = 1	L_f = 17	V_{ia} = 0.5
W_g = 17	L_3 = 3	D = 1.5

3. Filter analysis and modeling

Several basic equations should be recalled before delving into the SLR transmission line model to make filter analysis easier to understand. The equations given in [25] can be used to calculate the characteristic impedance of the microstrip line (Z_o) and effective dielectric constant (ε_{reff}). Moreover, the characteristic impedance with an input impedance (Z_{in}) of a lossless transmission line and a load impedance (Z_L) is provided in [26]. The phase constant (β) can be related to the resonant frequency of the transmission line using the following formula based on the quasi-TEM characteristic of the microstrip line [26].

$$\beta = 2\pi \times f_r \frac{\sqrt{\varepsilon_{reff}}}{c} \quad (1)$$

Where f_r is a resonant frequency, and c is the free space speed of light. Fig. 2 shows the even-mode and odd-mode equivalent circuit of the BPF.

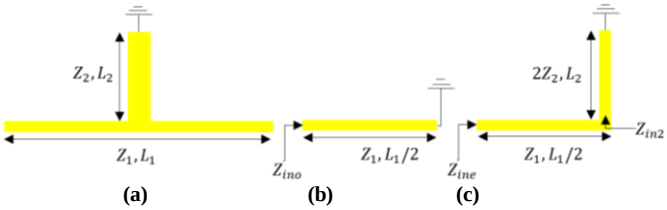

Fig. 2 (a) SL-MMR **(b)** even-mode equivalent circuit **(c)** odd-mode equivalent circuit.

Where Z_1 and Z_2 are the characteristic impedances of each section, L_1 and L_2 are length of the half wavelength open-circuited resonator and the quarter-wavelength short-circuited stub [27]. It is important to note that the even-odd modes resonant frequencies are obtained by producing a weak coupling between the feed line and the SL-MMR (E-shaped resonator) [28].

3.1. Odd-Mode Resonant Frequency

In the odd mode, two separate sources excite the dual ports of the filter. The signals have the same amplitude, but a 180° phase difference. In this situation, the voltage signals on the symmetry axis are of identical amplitude, but with a 180° difference in phases, and the current signals are equal in amplitude and phase [18]. Therefore, the resulting voltage at the axis of symmetry is equal to zero at the resonance frequency, but the current signal is at its maximum value as that in the short-circuit case. As illustrated in Fig. 2(c), the center stub effect is neglected due to this short circuit. The odd mode's input impedance is:

$$Z_{ino} = Z_1 \frac{Z_L + jZ_1 \tan\theta_1}{Z_1 + jZ_L \tan\theta_1} \tag{2}$$

Applying input impedance equation with $Z_L = 0$, results in:

$$Z_{ino} = jZ_1 \tan\theta_1 \tag{3}$$

Where θ_1 is the electrical length of the open-circuit stub which can be expressed as:

$$\theta_1 = \frac{\beta L_1}{2} \tag{4}$$

The condition of resonance is that the input impedance should equal to infinity $Z_{ino} = \infty$, at the resonant frequency [28]. Thus,

$$\theta_1 = (2n-1)\frac{\pi}{2}, \quad n = 1, 2, 3, \ldots. \tag{5}$$

By combining (5), (4) and (1), the odd-mode resonant frequency (f_{rodd}) can be obtained as follows:

$$f_{rood} = \frac{(2n-1)c}{2L_1\sqrt{\varepsilon_{reff}}} \tag{6}$$

where (ε_{reff}) is the effective dielectric constant of the feed line.

3.2. Even-Mode Resonant Frequency

In the even mode, two separate sources excite the dual ports of the filter. The signals have the same amplitude and phase difference. The voltage signals are identical in amplitudes and phase angles at the axis of symmetry, whereas the current signals are equal in amplitudes and are out of phase by [18]. A maximum voltage value is, therefore, displayed at the resonant frequency on the symmetry axis and a zero current value, which is comparable to the open circuit. The effect of the central stub appears in this situation, as illustrated in Fig. 2(b), and the symmetry axis divides the central stub into two halves.

$$Z_{in2} = 2Z_2 \frac{Z_L + jZ_1 \tan\theta_2}{2Z_2 + jZ_L \tan\theta_2} \tag{7}$$

For the short stub $Z_L = 0$,

$$Z_{in2} = j2Z_2 \tan\theta_2 \tag{8}$$

Where θ_2 is the electrical length of the short-circuit stub, which can be expressed as:

$$\theta_2 = \beta L_2 \tag{9}$$

The input impedance of the even mode is:

$$Z_{ine} = Z_1 \frac{Z_{in2} + jZ_1 \tan\theta_1}{Z_1 + jZ_{in2} \tan\theta_1} \tag{10}$$

For the resonant condition $Z_{ine} = \infty$, thus

$$Z_1 + jZ_{in2} \tan\theta_1 = 0 \tag{11}$$

Substituting (8) into (11) yields,

$$Z_1 - 2Z_2 \tan\theta_2 \tan\theta_1 = 0 \tag{12}$$

$$\tan\theta_2 \tan\theta_1 = \frac{Z_1}{2Z_2} \tag{13}$$

For simple case of $Z_1 = 2Z_2$, the above equation is reduced to:

$$\tan\theta_2 \tan\theta_1 = 1 \tag{14}$$

Therefore, the resonance condition for this simple case is given by:

$$\theta_1 + \theta_2 = (2n-1)\frac{\pi}{2} \tag{15}$$

or,

$$L_1 + 2L_2 = (2n-1)\frac{\pi}{\beta} \tag{16}$$

The even-mode resonant frequency f_{reven} for the case of $Z_1 = 2Z_2$ can thus be obtained as:

$$f_{reven} = \frac{(2n-1)c}{2(L_1 + 2L_2)\sqrt{\varepsilon_{reff}}} \tag{17}$$

From equations (6) and (17), the odd-mode resonant frequency is just affected by the length of the half-wavelength resonator (L_1), while the even-mode resonant frequency is not affected by both the central stub length (L_2) and (L_1). The effect of changing the length (L_2) is shown in Fig. 3(a). It is noticeable that when (L_2) is increased, the even-mode resonant frequency decreases, while the odd-mode resonant frequency is not affected so much. Fig. 3(b) shows the effect of changing (L_1) on both even-odd mode resonant frequencies, and it is clear that increasing the length of (L_1), both even-mode and odd-mode resonant frequencies will be decreased.

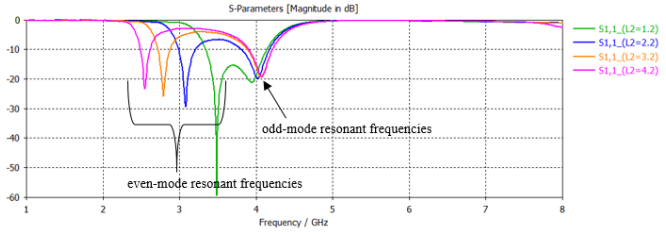

(a)

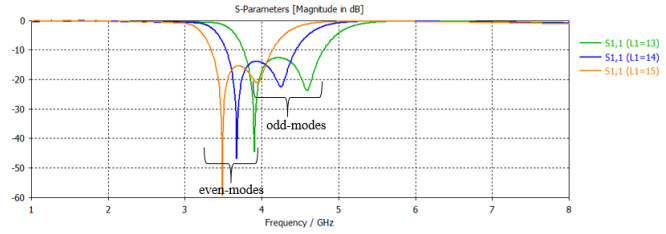

(b)

Fig. 3 even-odd mode resonant frequencies, **(a)** the effect of changing of (L_2), and **(b)** the effect of changing (L_1).

4. Simulation result

In this paper, the PIN diode (SMP1340-079LF) was selected to be the switching element used to reconfigure the BPF. The reflection and transmission coefficients of the proposed filter. The equivalent circuits of the PIN diode for the ON and OFF states using a characteristics impedance of 50 ohms on the dual ports are shown in Fig. 4, and their parameter values are given in Table 2. Advance Design System (ADS) 2020 [29] is used to simulate the corresponding equivalent circuit of PIN diodes, as shown in Fig. 4. PIN diodes are represented by lumped RLC elements in the ADS simulation to add and study the effect of actual PIN diodes. The insertion loss is 0.18 dB at the ON state, across the frequency range of 1 GHz to 8 GHz, as shown in Fig. 5(a). This indicates that the diode will have low impedance and operate as a short circuit for RF signals. When the PIN diode is turned OFF, the insertion loss will increase with the frequency, starting from a value of about 17 dB, as illustrated in Fig. 5(b). This will result in high impedance and no power from the source to the load terminal will be transmitted and it operates as an open circuit.

Table 2. the parameter values of the equivalent circuit of the PIN switch diode.

ON	OFF
Rs = 0.85 Ω	R = 103 Ω
L = 0.7 nH	L = 0.7 nH
	C = 0.21 pf

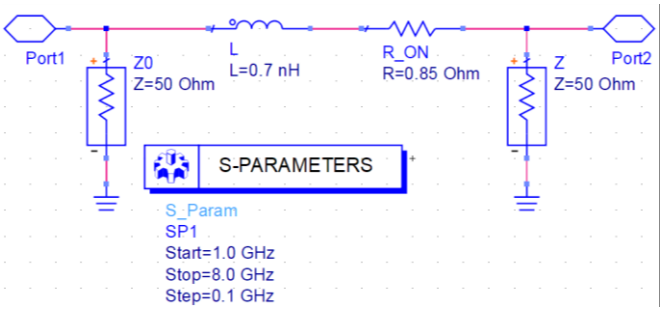

(a)

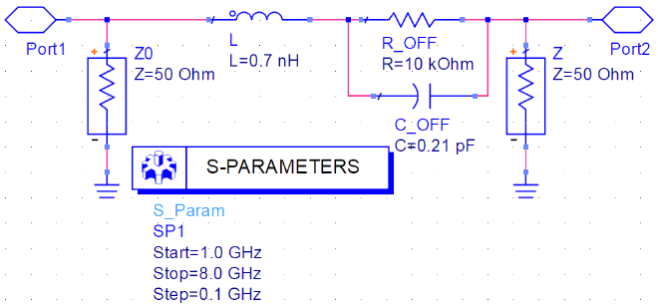

(b)

Fig. 4 equivalent circuit of PIN diodes, **(a)** ON state, **(b)** OFF state.

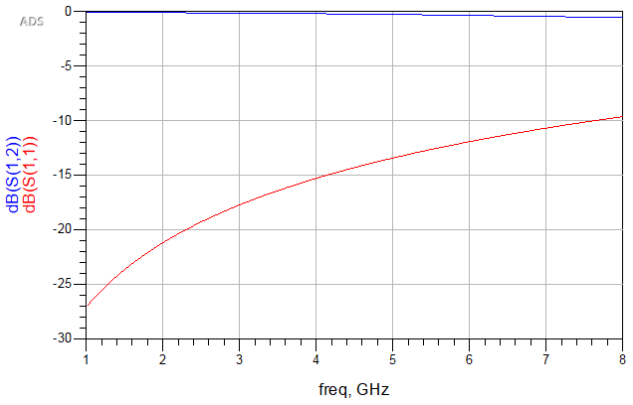

(a)

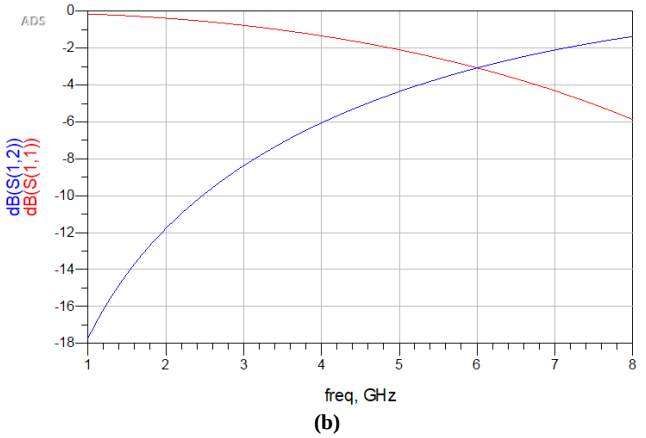

(b)

Fig. 5 S-Parameters of an equivalent circuit of PIN diodes, **(a)** ON state, **(b)** OFF state.

The simulated results of the BPF are summarized in two cases, depending on the state of the PIN diodes. CST Microwave Studio [30] is used to simulate the proposed BPF.

Case 1: (D1 & D2 are ON)

The BPF changes its operating band in response to the electrical length of the half-wavelength resonator when the pair of switch diodes is turned ON. In this case, the BPF covers the frequency range from 3.38 GHz to 3.95 GHz, which includes the WiMAX and 5G bands. The 3 dB fractional bandwidth (FBW) is equal to 16.2 % (absolute bandwidth = 570 MHz) with a mid-band insertion loss of 1.3 dB and a center frequency of 3.52 GHz. The reflection coefficient reaches a value of less than - 43 dB. The filter has two transmission zeros (T_{Zs}) in this case: the first one is at T_{z1} = 2.89 GHz with an insertion loss of more than 33 dB and the second one is at T_{z2} = 4.76 GHz with an insertion loss of more than 31 dB, as illustrated in Fig. 6.

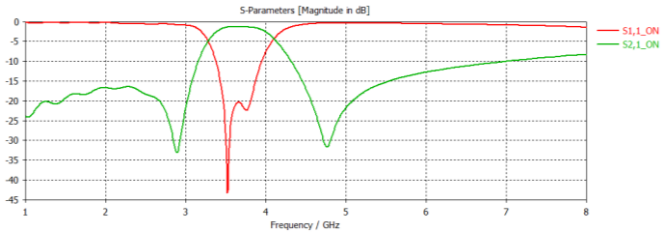

Fig. 6 S-parameter of the BPF at case 1.

Fig. 7 (a, b, and c) shows the surface current distribution of the BPF at the first transmission zero (T_{Z1}), center frequency (f_c) and the second transmission zero (T_{Z2}), respectively. It is clear that the current is concentrated at the E-shaped resonator at the frequencies of the transmission zeros, and there is no current at the output port. In adverse, the current passes through the filter directly to the output port at the filter's center frequency.

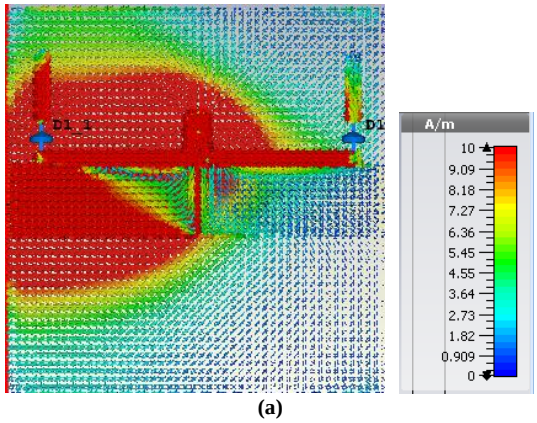

(a)

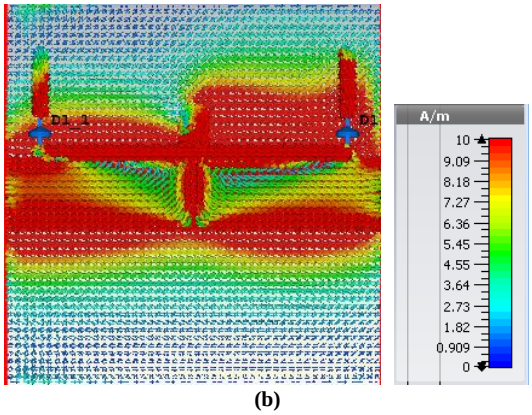

(b)

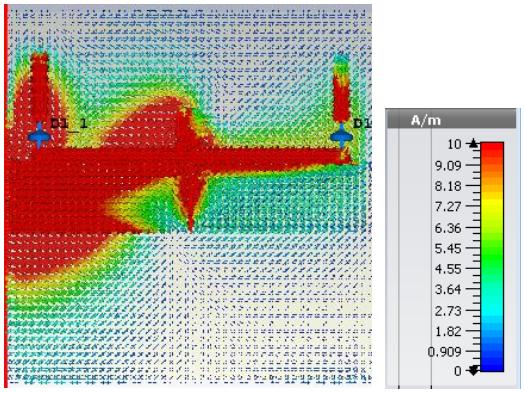

(c)

Fig. 7 surface current distribution at case 1. **(a)** T_{Z1} = 2.89 GHz, **(b)** f_c = 3.52 GHz, **(c)** T_{Z2} = 4.76 GHz.

Case 2: (D1 & D2 are OFF)

When the pair of switch diodes is turned OFF, the BPF changes its operating range to a higher frequency range because the length of the resonator is decreased. In this case, the coverage bandwidth is (4.7 - 5.93) GHz, including the WLAN band. The 3 dB fractional bandwidth (FBW) is 23.65% (absolute bandwidth = 1.23 GHz). The mid-band insertion loss is 0.8 dB, and the center frequency is 5.2 GHz with a reflection coefficient of less than - 28 dB. It also has two transmission zeros (T_{Zs}), the first one is at 3.65 GHz with an insertion loss of more than 47 dB and the second one is at 7.43 GHz with an insertion loss of more than 38 dB, as shown in Fig. 8.

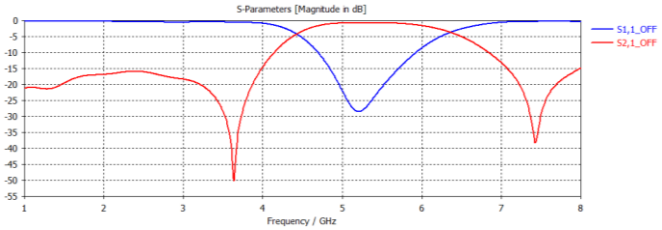

Fig. 8 S-parameters of the BPF at case 2.

The surface current distribution of the BPF at the first transmission zero (T_{Z1}), center frequency (f_c), and the second transmission zero (T_{Z2}), respectively, are shown in Fig. 9 (a, b, and c) respectively when the diodes are OFF.

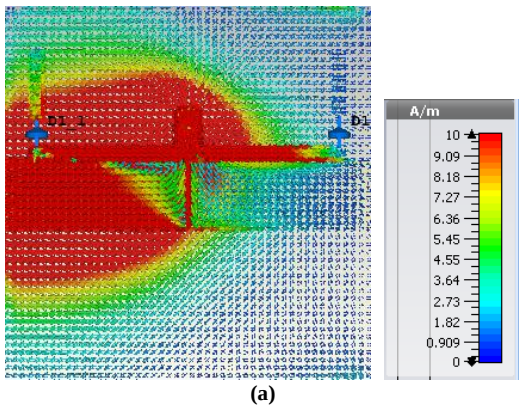

(a)

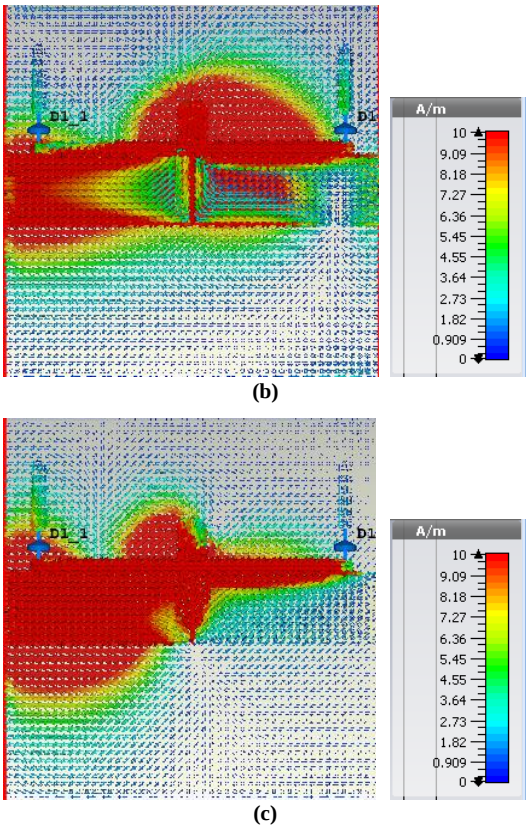

(b)

(c)

Fig. 9 Surface current distribution at case 2, **(a)** T_{Z1} = 3.65 GHz, **(b)** f_c = 5.2 GHz and **(c)** T_{Z2} = 7.43 GHz.

The reflection coefficient and the transmission coefficient of the reconfigurable BPF are shown in Fig. 10 (a and b), respectively, when the pair of PIN diodes is in ON-OFF states.

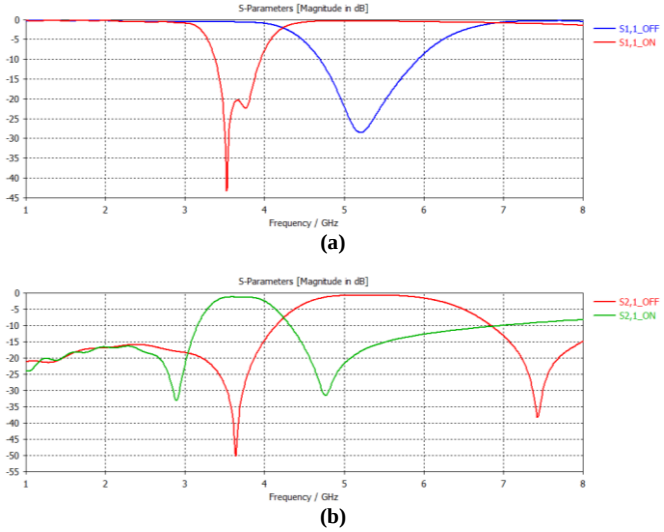

(a)

(b)

Fig. 10 S-Parameters for the two cases, **(a)** Reflection coefficient, **(b)** Insertion loss.

Table 3 shows the simulation results of the switchable BPF when a pair of PIN diodes is in ON-OFF states. Table 4 compared this work with some previous works. Low cost, small size and only a pair of PIN diodes are used in the proposed BPF with two tuning states to get two bands for WiMAX, 5G, and WLAN applications. Low insertion loss and high selectivity are obtained in each case with two transmission zeros characteristics of the bandpass filter.

Table 3. Simulation results of the proposed reconfigurable BPF.

Case	Band (GHz) (applications)	Center frequency f_c (GHz)	RL (dB) @ f_c	- 10 dB Impedance Bandwidth (MHz)	FBW %	IL (dB) @ (GHz)	Rejection (dB) @ f (GHz) (Transmission Zeros)	
							Lower Band	Upper Band
Case 1	3.38 - 3.95 (WiMAX)	3.52	43.35	570	16.2	33.16 @ 2.89 2.6 @ 3.38 1.3 @ f_c 2.1 @ 3.95 31.6 @ 4.76	33.16 @ 2.89 (T_{Z1})	31.6 @ 4.76 (T_{Z2})
Case 2	4.7 to 5.93 (5G and WLAN)	5.2	28.5	1230	23.65	47.6 @ 3.65 1.7 @ 4.7 0.8 @ f_c 1.4 @ 5.93 38.4 @ 7.43	47.6 @ 3.65 (T_{Z1})	38.4 @ 7.43 (T_{Z2})

Table 4. Comparison of the proposed work with other relevant works.

Ref.	Filter case	f_c (GHz)	FBW%	RL (dB)	IL (dB)	Via Holes	PIN diodes	Substrate	T_{Zs} GHz	No. of zeros	Size
[13]	*i*. Dual BPFs	1.2/3.5	3.5/4	34.4/32.3	2.79/2.96	2	2	RT/Duroid 6010LM εr = 10.2 h = 0.635	9.84 f_c	1	0.21 λg × 0.064 λg
	ii. BPF	1.2	3.5	34.4							
	iii. BPF	3.5	4	32.3							
[14]	*i*. BPF	2.4	58.5	More than 15	1.1	-	4	Roger 4003C εr = 3.55 h = 0.813 mm	2.7 f_c	1	0.514 λg × 0.514 λg = 0.264 λ_g^2
	ii. BPF	2.4	75								
[15]	*i*. BPF	5.69	34.8	More than 30	1.4	-	4	RO4003 εr = 3.38 h = 0.508 mm	-	2	29.4 mm × 29.4 mm
	ii. BPF	5.68	48.4							2	
	iii. WB-BPF	5.66	56.5							2	
[16]	Single-mode BPF	2.4	1.5	More than 15	1.5	-	2	32-mil thick RO4003C εr = 3.55	2.7	1	68 mm × 68 mm
	Dual-mode BPF	2.4	4.8		1.2				2.28 and 2.51	2	
[17]	*i*. BPF	2.4	20	More than 15	-	-	3	FR4 εr = 4.4 h = 0.8 mm	-	-	20 mm × 20 mm
	ii. BPF	3.5	11								
	iii. BPF	1.65-1.89	14								
This work	*i*. BPF (WiMAX)	3.52	16.2	43.35	1.3	1	2	FR4 εr = 4.3 h = 1.6 mm	2.89 and 4.76	2	0.36 λg × 0.36 λg = 0.1297 λ_g^2
	ii. BPF (5G, WLAN)	5.2	23.65	28.5	0.8				3.65 and 7.43	2	17 mm × 17 mm

5. Conclusions

A low-cost, compact reconfigurable bandpass filter is proposed in this paper. The bandpass filter effectively covers two frequency bands. A folded half-wavelength microstrip resonator loaded with a central stub has been used to construct an E-shaped filter. The frequency is reconfigured by inserting a pair of PIN diodes into a folded half-wavelength microstrip resonator. The first band is in the range of (3.38 - 3.95) GHz with a center frequency of 3.52 GHz, whereas the second is in the range of (4.7 - 5.93) GHz with a center frequency of 5.2 GHz, including WiMAX, 5G, and WLAN applications. The insertion losses of the two bands are 1.3 dB and 0.8 dB, respectively. The low insertion loss, high selectivity, compact size, and low cost make the proposed filter useful for communication filtenna in interweave cognitive radio applications.

References

[1] P. W. Wong and I. C. Hunter, "Electronically reconfigurable microwave bandpass filter", IEEE Transactions on Microwave Theory and Techniques, Vol. 57, Issue 12, pp. 3070-3079, 2009. https://doi.org/10.1109/TMTT.2009.2033883

[2] W. -H. Tu, "Switchable microstrip bandpass filters with reconfigurable on-state frequency responses", IEEE microwave and wireless components letters, Vol. 20, Issue 5, pp. 259-261, 2010. https://doi.org/10.1109/LMWC.2010.2045581

[3] A. M. Abbosh, "Design method for ultra-wideband bandpass filter with wide stopband using parallel-coupled microstrip lines", IEEE Transactions on microwave theory and techniques, Vol. 60, Issue 1, pp. 31-38, 2011. https://doi.org/10.1109/TMTT.2011.2175241

[4] F.-C. Chen, R.-S. Li, and Q.-X. Chu, "Ultra-wide stopband low-pass filter using multiple transmission zeros", IEEE Access, Vol. 5, pp. 6437-6443, 2017. https://doi.org/10.1109/ACCESS.2017.2693344

[5] J. Ni and J. Hong, "Compact varactor-tuned microstrip high-pass filter with a quasi-elliptic function response", IEEE transactions on microwave theory and techniques, Vol. 61, Issue 11, pp. 3853-3859, 2013. https://doi.org/10.1109/TMTT.2013.2281964

[6] Y. Wu, L. Cui, W. Zhang, L. Jiao, Z. Zhuang, and Y. Liu, "High performance single-ended wideband and balanced bandpass filters loaded with stepped-impedance stubs", IEEE Access, Vol. 5, pp. 5972-5981, 2017. https://doi.org/10.1109/ACCESS.2017.2695220

[7] K. M. F. Rabbi, "Miniaturised and reconfigurable planar filters for ultra-wideband applications", Ph.D. thesis, Faculty of Science and Technology, University of Westminster, 2014.

[8] Y. I. Al-Yasir, N. O. Parchin, Y. Tu, A. M. Abdulkhaleq, I. T. E. Elfergani, J. Rodriguez, and R. A. Abd-Alhameed, "A Varactor-Based Very Compact Tunable Filter with Wide Tuning Range for 4G and Sub-6 GHz 5G Communications", Sensors, Vol. 20, Issue 16, pp. 1-20, 2020. https://doi.org/10.3390/s20164538

[9] H. A. Atallah, A. B. Abdel-Rahman, K. Yoshitomi, and R. K. Pokharel, "Compact frequency reconfigurable filtennas using varactor loaded T-shaped and H-shaped resonators for cognitive radio applications", IET Microwaves, Antennas & Propagation, Vol. 10, Issue 9, pp. 991-1001, 2016. https://doi.org/10.1049/iet-map.2015.0700

[10] W.-J. Zhou and J.-X. Chen, "High-selectivity tunable balanced bandpass filter with constant absolute bandwidth", IEEE Transactions on Circuits and Systems II: Express Briefs, Vol. 64, Issue 8, pp. 917-921, 2016. https://doi.org/10.1109/TCSII.2016.2621120

[11] Y. Tawk, J. Costantine, and C. G. Christodoulou, "Reconfigurable filtennas and MIMO in cognitive radio applications" IEEE Transactions on Antennas and Propagation, Vol. 62, Issue 3, pp. 1074-1083, 2013. https://doi.org/10.1109/TAP.2013.2280299

[12] M. Donelli, M. Manekiya, and S. K. Menon, "Compact microstrip reconfigurable filter based on spiral resonators", Microwave and Optical Technology Letters, Vol. 61, Issue 2, pp. 417-424, 2019. https://doi.org/10.1002/mop.31587

[13] S.-C. Weng, K.-W. Hsu, and W.-H. Tu, "Compact and switchable dual-band bandpass filter with high selectivity and wide stopband", Electronics letters, Vol. 49, Issue 20, pp. 1275-1277, 2013. https://doi.org/10.1049/el.2013.2154
[14] S. Arain, P. Vryonides, M. A. B. Abbasi, A. Quddious, M. A. Antoniades, and S. Nikolaou, "Reconfigurable Bandwidth Bandpass Filter With Enhanced Out-of-Band Rejection Using π-Section-Loaded Ring Resonator", IEEE Microwave and Wireless Components Letters, Vol. 28, Issue 1, pp. 28-30, 2017. https://doi.org/10.1109/LMWC.2017.2776212
[15] T. Cheng and K.-W. Tam, "A wideband bandpass filter with reconfigurable bandwidth based on cross-shaped resonator", IEEE Microwave and Wireless Components Letters, Vol. 27, Issue 10, pp. 909-911, 2017. https://doi.org/10.1109/LMWC.2017.2746679
[16] P. Vryonides, S. Nikolaou, S. Kim, and M. M. Tentzeris, "Reconfigurable dual-mode band-pass filter with switchable bandwidth using PIN diodes", International Journal of Microwave and Wireless Technologies, Vol. 7, Issue 6, pp. 655-660, 2015. https://doi.org/10.1017/S1759078714000932
[17] J. Mazloum, A. Jalali, and M. Ojaroudi, "Miniaturized reconfigurable band-pass filter with electronically controllable for WiMAX/WLAN applications", Microwave and Optical Technology Letters, Vol. 56, Issue 2, pp. 509-512, 2014. https://doi.org/10.1002/mop.28101
[18] F. M. Alnahwi, Y. I. Al-Yasir, A. A. Abdulhameed, A. S. Abdullah, and R. A. Abd-Alhameed, "A Low-Cost Microwave Filter with Improved Passband and Stopband Characteristics Using Stub Loaded Multiple Mode Resonator for 5G Mid-Band Applications", Electronics, Vol. 10, Issue 4, pp. 1-15, 2021. https://doi.org/10.3390/electronics10040450
[19] J. Xu, W. Wu, and G. Wei, "Compact multi-band bandpass filters with mixed electric and magnetic coupling using multiple-mode resonator", IEEE Transactions on Microwave Theory and Techniques, Vol. 63, Issue 12, pp. 3909-3919, 2015. https://doi.org/10.1109/TMTT.2015.2488643
[20] D. Chen, H. Bu, L. Zhu, and C. Cheng, "A differential-mode wideband bandpass filter on slotline multi-mode resonator with controllable bandwidth", IEEE Microwave and Wireless Components Letters, Vol. 25, Issue 1, pp. 28-30, 2014. https://doi.org/10.1109/LMWC.2014.2370099
[21] J. Ai, Y. Zhang, K. Da Xu, D. Li, and Y. Fan, "Miniaturized Quint-Band Bandpass Filter Based on Multi-Mode Resonator and λ/4 Resonators with Mixed Electric and Magnetic Coupling", IEEE Microwave and Wireless Components Letters, Vol. 26, Issue 5, pp. 343-345, 2016. https://doi.org/10.1109/LMWC.2016.2549643
[22] S.-X. Zhang, Z.-H. Chen, and Q.-X. Chu, "Compact tunable balanced bandpass filter with novel multi-mode resonator", IEEE Microwave and Wireless components letters, Vol. 27, Issue 1, pp. 43-45, 2016. https://doi.org/10.1109/LMWC.2016.2629965
[23] Z. Wang, J. R. Kelly, P. S. Hall, A. L. Borja, and P. Gardner, "Reconfigurable parallel coupled band notch resonator with wide tuning range" IEEE Transactions on Industrial Electronics, Vol. 61, Issue 11, pp. 6316-6326, 2014. https://doi.org/10.1109/TIE.2014.2311386
[24] R. Zhou, I. Mandal, and H. Zhang, "Microwave bandpass filters with tunable center frequencies and reconfigurable transmission zeros", Microwave and Optical Technology Letters, Vol. 55, Issue 7, pp. 1526-1531, 2013. https://doi.org/10.1002/mop.27628
[25] R. Garg, I. Bahl, and M. Bozzi, Microstrip lines and slotlines, Third Edition, Artech house, 2013. ISBN:9781608075362
[26] D. M. Pozar, Microwave engineering, 4th Edition, John wiley & sons, 2011. ISBN: 978-0-470-63155-3
[27] X. Zheng, Y. Pan, and T. Jiang, "UWB bandpass filter with dual notched bands using T-shaped resonator and L-shaped defected microstrip structure", Micromachines, Vol. 9, Issue 6, pp. 1-11, 2018. https://doi.org/10.3390/mi9060280
[28] S. Sun and L. Zhu, "Capacitive-ended interdigital coupled lines for UWB bandpass filters with improved out-of-band performances", IEEE Microwave and Wireless Components Letters, Vol. 16, Issue 8, pp. 440-442, 2006. https://doi.org/10.1109/LMWC.2006.879492
[29] ADS: Advanced Design System, 2021.
[30] CST: Computer Simulation Technology Based on FIT Method, 2017.

Biographies

Yousif Mohsin Hasan received the B.Sc. degree in Electronic Engineering from the Department of Electronic Engineering, College of Electronics Engineering, University of Mosul, Mosul, Iraq, in 2006. He received the M.Sc. degree in "Electronics and Telecommunications Engineering" from the Faculty of Electrical Engineering, UTM, Malaysia, in 2015. He is currently a Ph.D. student at the Department of Electrical Engineering, College of Engineering, University of Basrah, Iraq. He worked as an Engineer in the College of Engineering, University of AL-Qadisiyah, Diwaniyah, Iraq from 2007 to 2012. He rejoined the College of Engineering, University of AL-Qadisiyah as an Assistant lecturer in 2015, then as a Lecturer from 2018 till now.

Abdulkareem S. Abdullah received the B.Sc. and M.Sc. degrees in Communication Engineering from the College of Engineering, University of Basrah, in 1980 and 1985 respectively. He received his Ph.D. degree in Electromagnetic Fields and Microwaves Technology from "Beijing University of Posts and Telecommunications (BUPT)" / Beijing / China in 2004. He also received a Post-doctor degree in Telecommunications Engineering from "Beijing Institute of Technology" / China in 2008. He is currently working as a professor at the Department of Electrical Engineering, College of Engineering, University of Basrah. He is a senior member of IEEE and has published more than 80 journal and conference papers. His research interest includes Antenna Design and Analysis, Smart Antennas, Microwaves Technology, Indoor and Outdoor Radio Waves Propagation.

Falih M. Alnahwi was born in Iraq on Jan. 9, 1983. He received a Ph.D. in Electrical and Computer Engineering from the University of Missouri-Columbia in the United States in 2015, while his B.Sc. and M.Sc. were granted by the University of Basrah in Iraq in 2004 and 2007 respectively. Since he completed his Ph.D., he has joined the faculty members of the Department of the Electrical Engineering at University of Basrah as a lecturer. His field of interest is antennas and wireless propagation especially the multiband, broadband, ultra-wide band antennas, Electromagnetic Fields, MIMO Systems, Metamaterial, mutual coupling reduction techniques, and reconfigurable antennas.